 DOI: 10.3217/978-3-85125-883-7-08

# NUMERICAL INVESTIGATION OF THE KORALM TUNNEL FIRE TESTS USING AN AUTONOMOUS MESHING APPROACH WITH ADAPTIVE MESH REFINEMENT

[1]Mathias Vångö, [1]Pietro Scienza, [2]Patrik Fößleitner, [3]Daniel Fruhwirt

[1]Convergent Science GmbH, AT,
[2] FVT mbH, AT, [3] Graz University of Technology, AT

## ABSTRACT

Understanding smoke propagation and temperature stratification in tunnels during fire incidents is crucial in order to ensure the road user's safety. To accurately predict these phenomena, numerical tools such as Computational Fluid Dynamics (CFD) are invaluable.

We present in this work a CFD model, which features an improved workflow and turnaround time by utilizing an autonomous mesh generation technology. A high-quality mesh is generated on the fly and enables the use of adaptive mesh refinement (AMR) based on local flow gradients.

To assess the proposed method, simulation results are compared with measurements from full-scale fire tests performed by the Institute of Thermodynamics and Sustainable Propulsion Systems (ITnA) at Graz University of Technology in the Koralm tunnel (Austria). Namely, temperature readings from several sensors were used as validation data, along with the observed maximum backlayering length.

*Keywords: CFD, autonomous mesh, adaptive mesh refinement, tunnel smoke propagation*

## 1. INTRODUCTION

Safety and risk-scenario assessments are key part of the design and certification for infrastructures such as road and railway tunnels. Computational Fluid Dynamics (CFD) could provide a suitable solution, avoiding the necessity to build physical models and allowing to test several different scenarios, even considering full scale conditions. Additionally, it allows to take a closer look to complex physical phenomena which are difficult to study otherwise.

To that end, Fruhwirt et al. [1] used numerical CFD simulations to assess fire and smoke propagation in the Austrian Koralm tunnel, validating the model against experimental data. Furthermore, Truchot et al. [2] simulated the venting of toxic gases from a truck loaded with batteries, and consequently the implications of the dangerous gas release and combustion inside a tunnel. Temperature profiles and smoke distribution were among the analyzed quantities.

Not only fire occurrences, smoke propagation and other hazardous conditions, but also mitigation scenarios are often addressed and modeled through CFD. On this line, Riess et al. [3] simulated the water mist spray from a fire extinguishing system on a burning area in different flow regimes.

Forced ventilation in tunnels is also a key topic of interest and CFD has been proven as a valuable tool to address such scenarios, being able to model turbulence, heat transfer and buoyancy [4]. This also applies in scenarios where the ventilation system has to handle smoke and fire occurrences. Sturm et al. [5] provide a precise and general insight of the ventilation control in case of a fire in a tunnel, while Khattri et al. [6] looked at the longitudinal ventilation, focusing on the oxygen content and its impact on the fire dynamics.

In this work, we introduce a numerical model intended to address these challenges, while keeping simplifications to the geometry to a minimum and overall improving the workflow. More specifically, we present a comparison between in-situ measurements from the Koralm tunnel presented by Fruhwirt et al. [1] and numerical results obtained by our model. This comparison serves as validation of the model for the complex near-fire region, in the case of a longitudinally well-ventilated fire situation.

## 2. COMPUTATIONAL MODEL

In this work, we used CONVERGE [7] version 3.0.19 for all the simulations. A fully compressible URANS (Unsteady Reynolds-Averaged Navier-Stokes) methodology was employed using the well-known two-equation standard k-ε model, along with the real gas Redlich-Kwong equation of state. A second-order central difference spatial discretization scheme was employed, and a modified SIMPLE (Semi-Implicit Method for Pressure-Linked Equations) algorithm was used to solve the pressure velocity coupling. Although CONVERGE have not previously been used for large scale fire simulations, it has been extensively used and validated in other application areas, such as internal combustion engines, gas turbines as well as pumps and compressors [8, 9, 10]. Detailed descriptions of the governing equations and numerics are given in Richards et al. [11].

### 2.1. Physical models

Although CONVERGE possesses capabilities to model combustion by directly solving detailed chemical reaction mechanisms, we employed in this work the Eddy Dissipation combustion model (EDM) [12], which has been found reasonable considering computational cost and accuracy tradeoff.

Radiation was accounted for by solving the radiative transfer equation (RTE) using the Discrete Ordinates Method (DOM). Typically for large-scale fire simulations the flame temperatures are not properly resolved due to prohibitive computational expense, hence we applied the Optically-Thick, Specified Radiative Fraction model [13] to scale the radiative emission at the flame based on a pre-determined, user-specified radiative fraction.

In order to accurately model the wall heat transfer, we incorporated the solids into our model through the Conjugate Heat Transfer (CHT) method. Two CHT models were used, 3D-CHT and 1D-CHT, where the former includes the solid walls in the computational domain, and the latter uses virtual one-dimensional layers normal to the wall boundary.

### 2.2. Mesh

CONVERGE uses a modified Cartesian cut-cell meshing method which allows to retain the real geometry details without introducing any modification to the boundary shape. In this framework, the mesh generation process is fully automated and the grid is regenerated every time step, thus allowing moving and deforming boundaries. Furthermore, in traditional CFD, *a priori* knowledge of local flow features is often required to achieve satisfactory results, which is especially challenging in complex scenarios. As the mesh is continuously updated in CONVERGE, the mesh is allowed to be locally refined during runtime using the Adaptive Mesh Refinement (AMR) approach. More precisely, AMR evaluates the magnitude of the sub-grid field $\phi'$ of user-specified variables (e.g., temperature and velocity) to assess if mesh refinement should be applied, satisfying user defined criteria. $\phi'$ is defined as $\phi' = \phi - \bar{\phi}$, where $\phi$ and $\bar{\phi}$ are the actual and resolved field respectively.

The sub-grid field is approximated as the second order derivative

$$\phi' = -\alpha_{[k]} \frac{\partial^2 \bar{\phi}}{\partial x_k \partial x_k}, \quad (1)$$

arising from an infinite series expression of $\phi'$, where, $\alpha_k$ is $(\Delta x_k)^2/24$ for rectangular shaped cell. This methodology allows the mesh to be refined only when and where necessary, making optimal use of the cell count.

## 3. FIRE TEST DESCRIPTION

As means for validation of our approach we use the full-scale fire tests performed by ITnA in the Koralm tunnel, Austria. The aim of these tests was primarily to study smoke propagation to obtain information on keeping escape routes free of smoke. Hence, temperature measurements were taken at several locations downstream of the fire location, as well as the upstream smoke propagation (backlayering) length was measured.

In these tests, fire pools were used as fire source, placed in a protective fire box within the tunnel as shown in Fig. 1. Fourteen fire tests were performed with varying test duration and fire intensities. In this work, we focused on one particular test with eight pool fires giving approximately 18 MW sustained intensity, with a burn duration of eight minutes. For a detailed description of the fire tests see Sturm et al. [14].

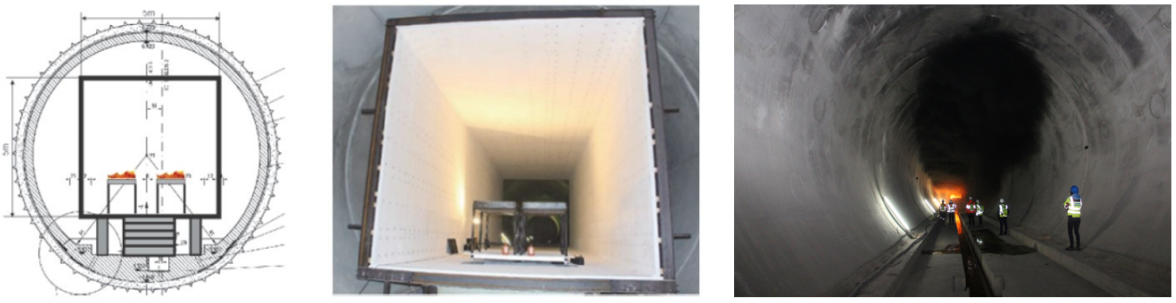

Figure 1: Visualization of the test pool fire setup and the protective box.

During the tests, many temperature measurements were taken. In this work, we used the temperature measurements obtained from the sensor arrays MP5 and MP6, as illustrated in Fig. 2, to evaluate the simulated temperature stratification. Furthermore, a comparison of the concrete temperature was carried out with sensor S7.1 and S7.2, as well as with the maximum observed backlayering length from the test.

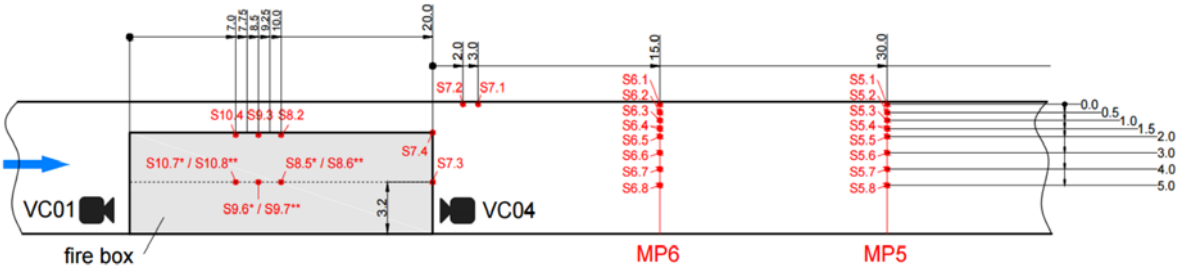


Figure 2: Temperature sensors locations within the test configuration.

## 4. SIMULATION SETUP

In order to evaluate our approach, we aimed to replicate the test case scenario described above within the numerical framework.

### 4.1. Simulation domain and mesh settings

The domain used for the simulations is shown in Fig. 3. It can be noted that little to no simplifications has been made to the geometry, as it includes the correct cross-section profile of the tunnel, the detailed fire box, as well as the solid concrete tunnel wall.

Determining the correct mesh size is not trivial in CFD, but the characteristic fire diameter

$$D^* = \left( \frac{\dot{Q}}{\rho c_p T \sqrt{g}} \right)^{\frac{2}{5}}, \tag{2}$$

is often used in this context as a comparative length scale to define how well the flow is resolved [10]. Here, $\dot{Q}$, $\rho$, $c_p$, $T$ and $g$ refer to fire heat release rate, density, specific heat, temperature and gravity respectively. In this work, we used a relatively coarse mesh size of $\Delta x = D^*/5$ towards the ends of the tunnel, whereas the centre part of the tunnel, close to the fire, was refined to $\Delta x = D^*/10$. The grid was further refined in the direct vicinity of the fire source with the size $\Delta x = D^*/40$ using AMR based on temperature.

Consequently, the coarsest element size was 0.6 m, while the fire zone was refined with AMR using 0.075 m cells. Furthermore, in order to capture the strong temperature gradient close to the wall, additional fixed local refinement at the tunnel wall was applied via a boundary fitted grid, extruded from the surface with the first layer height being 0.01 m, an expansion ratio of 1.5 and a total of seven layers. The total cell count ranged from approximately 800 000 to 950 000 during the simulation due to AMR. The mesh used in the center part of the tunnel is visualized in Fig. 4.

The chosen mesh element size was rather small according to similar studies, as achieving mesh independence is in general challenging for large scale fire simulations, with temperature over-prediction being common for too coarse meshes [15]. We did however compare with a near-fire mesh of $\Delta x = D^*/30$ and $\Delta x = D^*/60$, but concluded that the chosen mesh resolution was sufficient for this study.

### 4.2. Boundary conditions

As boundary condition for the tunnel supply air velocity, we used the temporally varying profile measured in the fire test, ranging between 1.2 and 2.5 m/s. The fire size was imposed based on the measured fuel consumption rate of approximately 0.4 kg/s during the sustained burn phase. More specifically, the temporally noisy measured fuel consumption rate was approximated as a fitted polynomial, as shown in Fig. 5, and imposed as a fuel inflow rate at the fire pool patches.

In the experiment, a mixture of diesel and gasoline was used as fuel, whereas in our simulation we used pure isooctane with a specified lower heating value (LHV) of 42.2 MJ/kg based on the fuel mixture. Furthermore, a specified radiative fraction of 0.4 was used together with yield factors 0.1 and 0.001 $kg/kg_{fuel}$ for CO and soot respectively.

Due to the relatively thin layer of protective material in the fire box, the fire box walls were modelled using 1D-CHT. Material properties of Promatect-T were used and the wall thickness was divided into 20 evenly-spaced layers.

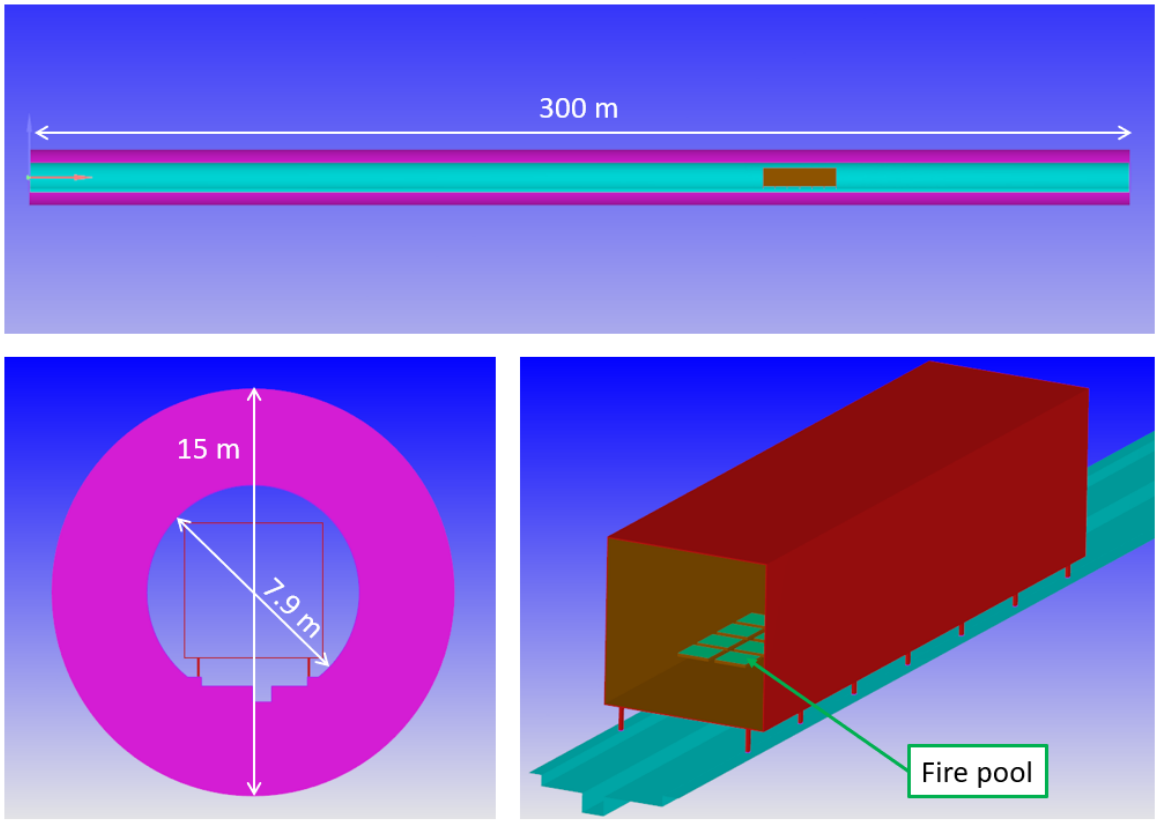


Figure 3: Simulation domain visualization. The top image is showing a clipped view at the centerline along the x-axis, the bottom left the tunnel cross section and the bottom right a zoom of the fire box.

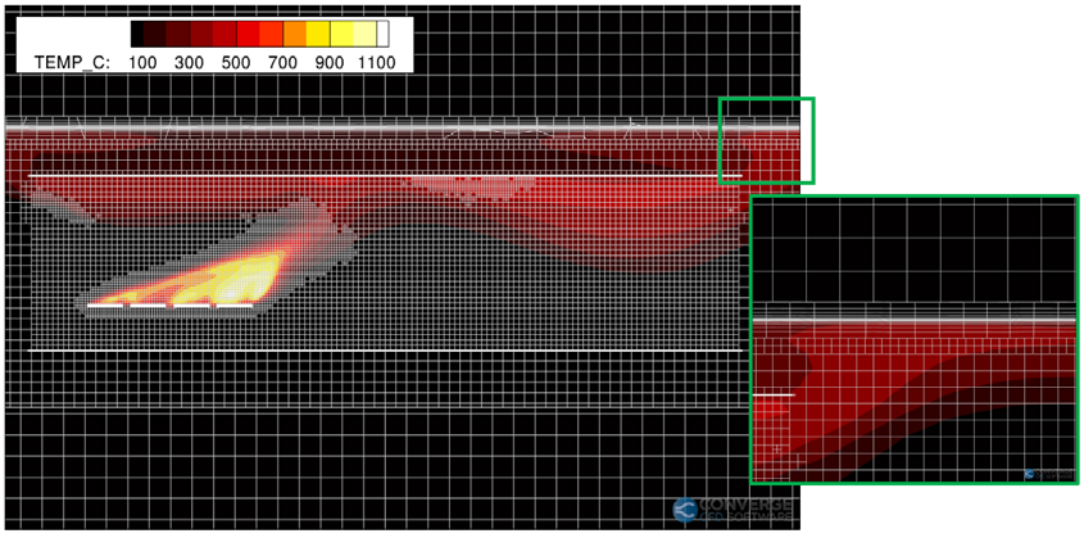


Figure 4: Visualization of the computational mesh in the center part of the tunnel.

## 5. RESULTS

In this section we present our findings from the previously described simulations. Figures 6 and 7 show the temperature stratification at various times at temperature sensor arrays S5 and

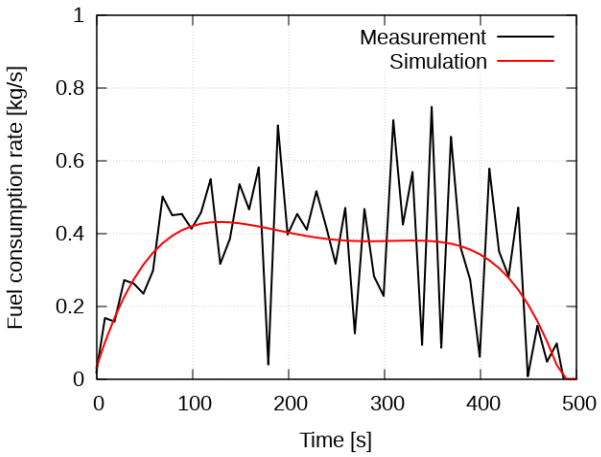


Figure 5: Comparison of the fuel consumption rate used in the simulation and the measured one from the fire test.

S6 respectively, for the measured values from the fire test (left) and simulation (right). In general, the trends and temperature magnitudes are well captured, especially in the upper part of the tunnel where hot smoke is present. This suggests that the downstream smoke propagation was adequately predicted and that the chosen methodology for the fire dynamics and radiative behaviour are well represented. The temperature gradient close to the upper wall is also adequately captured by the simulation when compared to the measurement. This indicates that the near-wall mesh strategy allows to satisfactorily capture the wall heat transfer. It should be noted that the temperature gradient at the upper wall is large and the temperature obtained in that region is highly sensitive to the exact sensor location, which is difficult to perfectly replicate in the simulation.

Figure 8 visualizes the concrete surface temperature at sensor location S7.1 and S7.2, which further indicate that the wall heat transfer trend is reasonably captured, although some underprediction of the temperature can be observed. Similarly here, the results experience high sensitiviy to the sensor location, so it's difficult to precisely determine the cause of the observed surface temperature differences. To fully understand that behavior, more specific tests would need to be conducted which was outside the scope of this work, as the primary focus was the smoke propagation.

Furthermore, the simulated backlayering length was compared with the carried out measurements. As no time history of the backlayering length was available from the fire tests, the maximum observed backlayering are compared and presented in Table 1. Also here a satisfactory agreement can be observed.

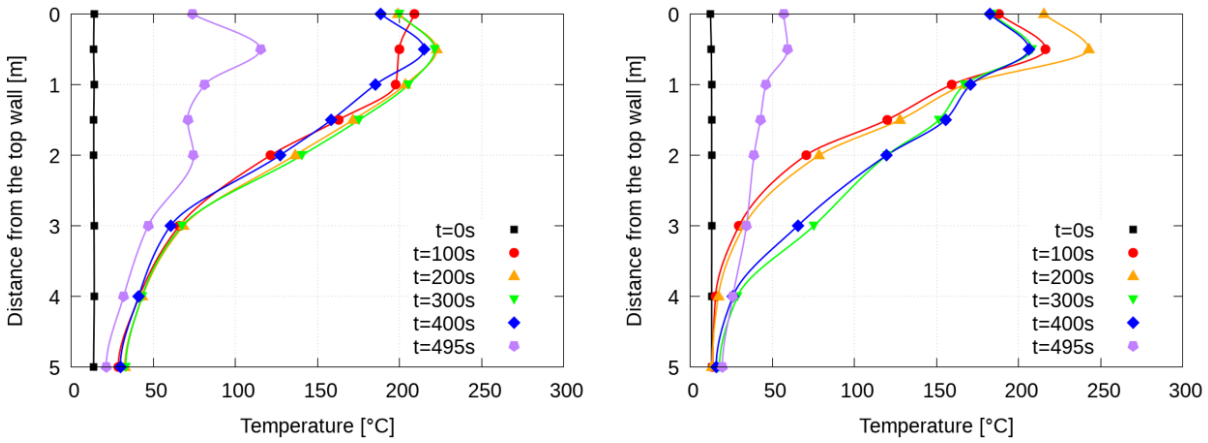


Figure 6: Vertical temperature profiles at sensor location S5 from measurement (left) and simulation (right) at various times.

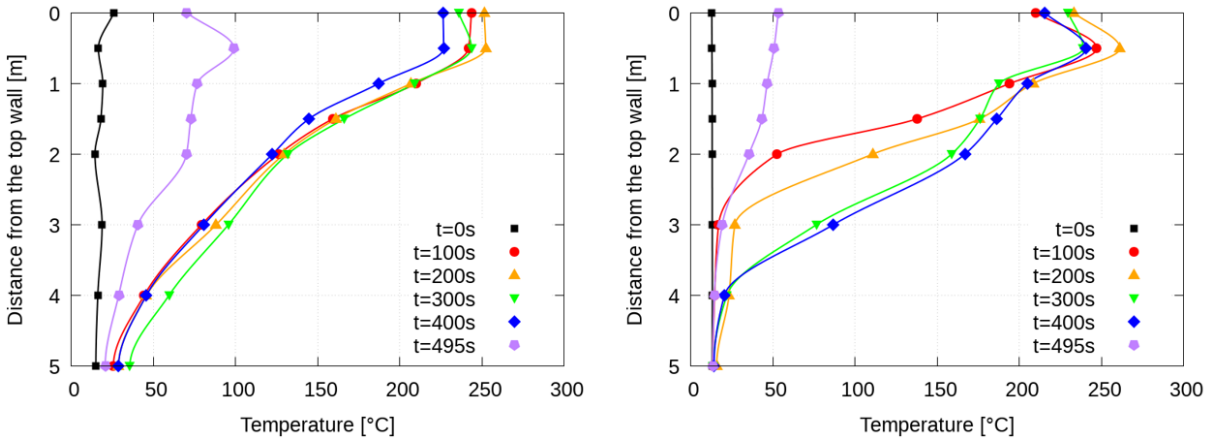


Figure 7: Vertical temperature profiles at sensor location S6 from measurement (left) and simulation (right) at various times.

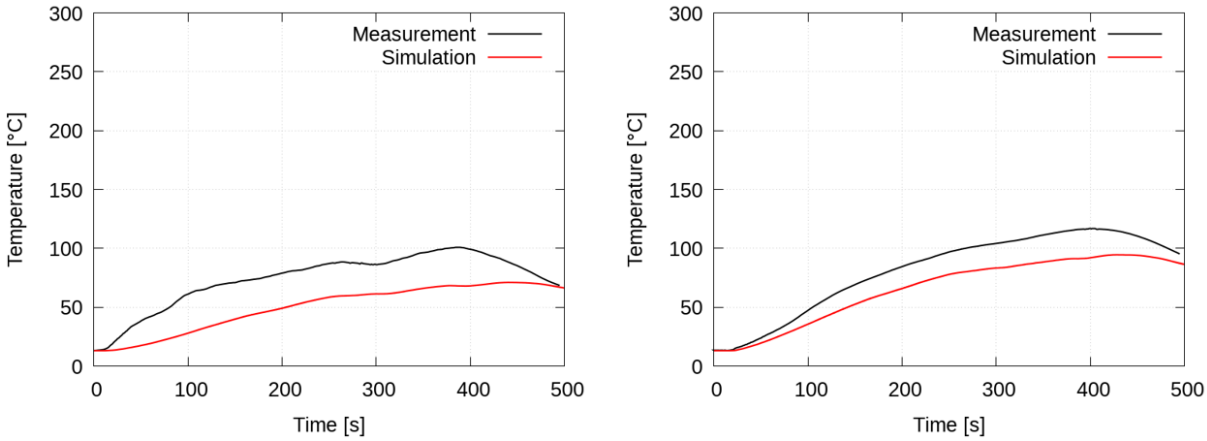


Figure 8: Comparison of the concrete temperature at sensor S7.1 (left) and S7.2 (right) between measurement and simulation.

Table 1: Comparison of the maximum observed backlayering length between the simulation and measurement.

| | **Measurement** | **Simulation** |
|---|---|---|
| **Backlayering length** | 160 m | 155 m |

## 6. CONCLUSION

In this work, we have presented a numerical model using a truly autonomous mesh approach to simulate large scale fire scenarios, intended to accurately predict smoke propagation during fire incidents to ensure smoke free evacuation paths. The chosen numerical strategy for important physical phenomena was presented, along with a discussion of necessary simplifications and special modelling requirements for this particular application.

The model was validated against real fire tests carried out by ITnA in the Austrian Koralm tunnel, where several measurements for both downstream and upstream smoke propagation were taken. Namely, downstream temperature stratification and concrete surface temperatures were directly compared with measurements from temperature sensors, as well as the maximum backlayering length was compared with observations from the fire test.

Generally, the simulation showed good agreement with the measured data. The downstream temperature stratification was well represented, showing very reasonable magnitudes with the exception of a slight underprediction for the lower part of the tunnel. We did also see some

underprediction of the concrete surface temperature, although it should be noted that the exact sensor location was of great importance due to the strong temperature gradient observed in the vicinity of the wall. Additionally, the observed backlayering length was in good agreement, further highlighting the accurate capturing of the smoke propagation, suggesting that the chosen numerical approach could be a relevant tool in fire safety scenarios.

## 7. REFERENCES


1. Fruhwirt, D., Sturm, P., Bacher, M., & Schwingenschlögl, H. (2020). Smoke propagation in tunnels-comparison of in-situ measurements, simulation and literature. In *10th International Conference Tunnel Safety and Ventilation*.
2. Truchot, B., Leroy, G., & Marlair, G. (2016). CFD and engineering method coupling for evaluating the fire relative to battery transportation. In *8. International Conference on Tunnel Safety and Ventilation* (pp. 132-140).
3. Riess, I., & Steck, M. (2018). On the aerodynamics of water mist from a ventilation designer's perspective. In *International Conference Tunnel Safety and Ventilation, Graz*.
4. Fleming, & C., Rhodes, N. (2018). A validation of the fire dynamics simulator for smoke dispersion from metro stations. In *International Conference Tunnel Safety and Ventilation, Graz*.
5. Sturm, P., Beyer, M., & Rafiei, M. (2017). On the problem of ventilation control in case of a tunnel fire event. *Case Studies in Fire Safety*, *7*, 36-43.
6. Khattri, S. K., Log, T., & Kraaijeveld, A. (2019). Tunnel fire dynamics as a function of longitudinal ventilation air oxygen content. *Sustainability*, *11*(1), 203.
7. Richards, K. J., Senecal, P. K., and Pomraning, E., CONVERGE 3.0, Convergent Science, Madison, WI (2022)
8. Senecal, P. K., Pomraning, E., Richards, K. J., & Som, S. (2012). Grid-convergent spray models for internal combustion engine CFD simulations. In *Internal Combustion Engine Division Fall Technical Conference* (Vol. 55096, pp. 697-710). American Society of Mechanical Engineers.
9. Li, Y., Rowinski, D. H., Bansal, K., & Rudra Reddy, K. (2018). CFD modeling and performance evaluation of a centrifugal fan using a cut-cell method with automatic mesh generation and adaptive mesh refinement.
10. Omote, H., Hirota, K., Hotta, T., Kumar, G., & Drennan, S.A (2015). Combustion and Conjugate Heat Transfer CFD Simulations to Support Combustor Design. In *International Gas Turbines Conference*, Tokyo, Japan.
11. Richards, K. J., Senecal, P. K., and Pomraning, E., CONVERGE 3.0 Manual, Convergent Science, Madison, WI (2022)
12. Magnussen, B. F., & Hjertager, B. H. (1977). On mathematical modeling of turbulent combustion with special emphasis on soot formation and combustion. In *Symposium (international) on Combustion* (Vol. 16, No. 1, pp. 719-729). Elsevier.
13. McGrattan, K., Hostikka, S., McDermott, R., Floyd, J., Weinschenk, C., & Overholt, K. (2013). Fire dynamics simulator user's guide. *NIST special publication*, *1019*(6), 1-339.
14. Sturm, P., Rodler, J., Thaller, T., Fruhwirt, D., & Fößleitner, P. (2019). Hot smoke tests for smoke propagation investigations in long rail tunnels. *Fire safety journal*, *105*, 196-203.
15. Vigne, G., & Jonsson, J. (2009). Experimental research–large scale tunnel fire tests and the use of CFD modelling to predict thermal behaviour. In *Advanced Research Workshop on Fire Protection and Life Safety in Buildings and Transportation Systems*, Santander, Spain (pp. 255-272).